Ab-initio take on effective single-particle energies in doubly closed shell nuclei

T. Duguet[1, 2, *] and G. Hagen[3, 4, †]

[1]CEA-Saclay DSM/Irfu/SPhN, F-91191 Gif sur Yvette Cedex, France
[2]National Superconducting Cyclotron Laboratory and Department of Physics and Astronomy,
Michigan State University, East Lansing, MI 48824, USA
[3]Physics Division, Oak Ridge National Laboratory, Oak Ridge, TN 37831, USA
[4]Department of Physics and Astronomy, University of Tennessee, Knoxville, TN 37996, USA
(Dated: October 17, 2011)

The present work discusses, from an ab-initio standpoint, the definition, the meaning, and the usefulness of effective single-particle energies (ESPEs) in doubly closed shell nuclei. We perform coupled-cluster calculations to quantify to what extent selected closed-shell nuclei in the oxygen and calcium isotopic chains can effectively be mapped onto an effective independent-particle picture. To do so, we revisit in detail the notion of ESPEs in the context of strongly correlated many-nucleon systems and illustrate the necessity to extract ESPEs through the diagonalization of the centroid *matrix*, as originally argued by Baranger. For the purpose of illustration, we analyse the impact of correlations on observable one-nucleon separation energies and non-observable ESPEs in selected closed-shell oxygen and calcium isotopes. To further qualify the meaning and usefulness of ESPEs, we quantify the resolution-scale dependence of ESPEs and establish to what extent the first 2^+_1 excitation energy is correlated with the size of the gap at the Fermi energy in ESPE and one-nucleon separation energy spectra.

I. INTRODUCTION

The concept of single-nucleon shells dates back to the early days of nuclear physics and constitutes the basic pillar of the nuclear shell model [1]. The independent-particle approximation provides a zeroth-order picture of the structure of nuclei on top of which correlations are added to provide a more realistic description. Based on such a rationale, the correlated shell model has been able to explain the occurrence of extraordinarily stable configurations for specific neutron and proton numbers, known as magic numbers. As a matter of fact, the universal character of such magic numbers over the nuclear chart remains an open question today. Recently, the evolution of shell structure and the understanding of the neutron drip-line location in oxygen isotopes have received considerable experimental and theoretical attention [2–4], e.g. significant shell gaps have been identified in ^{22}O and ^{24}O leading to the interpretation of new magic shell closures at $N = 14, 16$ in $Z = 8$ nuclei.

Identifying the underlying mechanisms responsible for the occurrence or the disappearance of magic numbers in specific regions of the nuclear chart requires improvement on the traditional shell model by allowing for a more systematic and consistent inclusion of correlations. In particular, questions related to the impact of continuum degrees of freedom [5–7] and of three-nucleon forces on the evolution of nuclear shells is a frontier driving low-energy nuclear physics research in connection with radioactive ion beam facilities [4, 8, 9].

Whether a certain nucleon number qualifies as a (new) magic number cannot be postulated a priori. Experimentally, several quantities, e.g. the excitation energy and the collective character of the first 2^+ state in even-even isotopes, the size of the gap in the one-nucleon addition/removal spectrum, and the spectroscopic factors of associated low-lying states in odd-even neighbours need to be extracted in order to make such an assessment. Theoretically, the same quantities need to be computed while including all many-body correlations that could play a role in order to check whether the picture associated with a magic number eventually holds.

It can be useful in this context, for analysis and interpretation purposes, to extract a single-nucleon shell structure, i.e. a set of *effective* single-particle energies (ESPEs) associated with an underlying independent-particle-like picture the system is mapped on. However, immediate non-trivial questions arise that are at the heart of the present study

1. How can a single-nucleon shell structure be meaningfully and unambiguously defined in a system that is intrinsically correlated; i.e. in which way are ESPEs extracted from (correlated) observables?

2. Correspondingly, to which auxiliary independent-particle problem are ESPEs related, i.e. which one-body Hamiltonian are ESPEs the eigenvalues of?

3. Is it necessary to access the fully correlated description to extract ESPEs? If so, to what extent do correlations impact the effective independent-particle picture provided by such ESPEs?

4. In which way are ESPEs related to underlying nuclear forces?

5. Given that ESPEs can be extracted unambiguously, is the associated simplified picture needed and beneficial or potentially misleading? In other words,

*Electronic address: thomas.duguet@cea.fr
†Electronic address: hageng@ornl.gov

can the behaviour of actual observables, e.g. one-nucleon separation energies or excited 2^+ energies, be inferred unambiguously from the ESPE spectrum? In particular, what patterns can the ESPE spectrum be expected to display in a particularly stable nucleus, i.e. in a magic nucleus?

Several of the above questions have been answered long ago while others still necessitate further clarifications. The procedure to extract ESPEs unambiguously (cf. point 1 above) goes back to French and Baranger [10–12] and can be utilized to address points 2, 3, 4, and 5. Such a procedure defines ESPEs as *centroid* energies denoting barycenters of *a priori correlated* total binding energy differences between the A-nucleon state the one-nucleon transfer is performed on and the complete set of eigenstates of the A+1 and A-1 systems. Eventually, centroids can be related [11–13] to the monopole part [14, 15] of underlying nuclear interactions, which effectively answers point 4 above.

In spite of the existence of an unambiguous procedure to compute ESPEs, difficulties exist that can lead to improper conclusions, e.g. conclusions based on an analysis whose model dependence has not been properly identified and stated. On the experimental side, extracting a centroid energy necessitates the identification of all many-body states with a given J^π from both one-nucleon stripping *and* pick-up reactions, which is not often possible. This is particularly critical as one moves away from doubly closed shell nuclei.

Theoretically, various levels of model dependence arise in the computation of ESPEs. On the deepest level, it is essential to understand that ESPEs depend, contrary to true observables, on the resolution scale Λ used to define and solve the nuclear many-body problem. As a result, changing Λ through, e.g., a unitary transformation on Fock space, changes ESPEs while leaving actual observables invariant. In this sense ESPEs are similar to spectroscopic factors; i.e. they can be used as a Λ-dependent analysis tool but cannot be seen as fundamental observable quantities. Moreover, and on a less fundamental level, approximations are often introduced in the computation of ESPEs that generate an artificial dependence on the single-particle basis used. These various points will be discussed and illustrated in the present paper.

Difficulties may also arise when comparing ESPEs computed from an ab-initio approach on the one hand and from more effective methods, e.g. shell model and energy density functional, on the other. For instance, while the empirical shell-model "anchors" ESPEs on one-nucleon addition (removal) energies to (from) the closed-shell core nucleus of reference, this is not the case in an ab-initio context, as will be illustrated below.

The present paper follows the approach by Baranger as a way to delve further into the meaning and the usefulness of ESPEs by addressing questions 2, 3 and 4 above, as well as by quantifying the error made when using approximations to the Baranger definition. The paper is organized as follows. Section II collects essentially known results regarding the definition and the computation of ESPEs. Such a rather exhaustive introductory part is needed to discuss points that have often been overlooked over the years. Section III details the computation of ESPEs within the frame of the coupled-cluster (CC) method. Section IV reports our results and illustrates various key properties of ESPEs. Specifically, the effect of correlations on one-nucleon separation energies and on ESPEs discussed focusing first on a few specific examples before addressing systematics in oxygen and calcium isotopes. Starting from the ab-initio perspective provided by our results, the rationale behind the truncated shell model is then briefly justified. Next, errors made by computing ESPEs in approximate ways are addressed before illustrating the deeper model dependence of ESPEs associated with their intrinsic resolution scale dependence. Eventually, the (lack of) correlation between the excitation energy of the first 2_1^+ state and the size of the gap in both ESPE and separation energy spectra is analysed. Conclusions are given in Sec. V.

II. EFFECTIVE SINGLE-PARTICLE ENERGIES

In low-energy nuclear structure theory, one usually starts from an independent-particle model to convey the basic notions of single-particle states and shell structure. In this context, one resorts to systems that can be postulated *a priori* as being little influenced by correlations such that an effective independent-particle picture can be safely used. In a second step, actual correlations are introduced to explain, e.g., the fragmentation of the single-particle strength visible in one-nucleon transfer reactions. Such a pedagogical presentation makes it difficult to picture the possibility to define and extract *a posteriori* an *effective*, underlying single-particle shell structure in the presence of correlations, i.e. for A-body systems that are, strictly speaking, always correlated. It is thus more instructive to start from a realistic picture of the nucleus, i.e. a rather strongly correlated system, and extract a posteriori an effective single-particle shell structure from which correlations are to a large extent, but not entirely, screened out [11].

To do so, we introduce the nuclear Hamiltonian under the form[1] $H = T + V^{2\mathrm{N}} + V^{3\mathrm{N}} + \ldots$, where T denotes the kinetic energy operator while $V^{B\mathrm{N}}$ corresponds to a B-body interaction. We limit ourselves to 2N and 3N interactions throughout the formal part of the paper and to 2N forces in actual applications. Studying the impact

---

[1] The complication associated with the self-bound character of the nucleus, i.e. the need to subtract the center-of-mass motion in order to deal with internal many-body states and eigenenergies [16], is overlooked in the present paper. Dealing with this difficulty in actual calculations is mandatory but would unnecessarily complicate the analytical expressions presented here without modifying significantly the outcome.

of 3N interactions and forces of higher rank is postponed to future works. Given H, eigenstates and eigenenergies of the A-nucleon system are obtained by solving

$$H|\Psi_\mu^A\rangle = E_\mu^A|\Psi_\mu^A\rangle \ , \tag{1}$$

where the symmetry quantum number denoting the particle number has been singled out. The label μ collects a principal quantum number n_μ, total angular momentum J_μ, the projection of the latter along the z axis M_μ, parity Π_μ and isospin projection along the z axis T_μ of the many-body state of interest. Use of the Greek label κ_μ will be made to denote the subset of quantum numbers $\kappa_\mu \equiv (\Pi_\mu, J_\mu, T_\mu)$. Due to rotational invariance of the nuclear Hamiltonian, eigenenergies $E_\mu^A \equiv E_{n_\mu \kappa_\mu}^A$ are independent of M_μ.

In the following, we consider a spherical single-particle basis $\{a_p^\dagger\}$ appropriate for discussing *spherical* shell structure. Basis states are labelled by $p \equiv \{n_p, \pi_p, j_p, m_p, \tau_p\} \equiv \{n_p, m_p, \alpha_p\}$, where n_p represents the principal quantum number, π_p the parity, j_p the total angular momentum, m_p its projection along the z-axis, and τ_p the isospin projection along the same axis.

We also consider the direct-product basis $\{b_{\vec{r}\sigma\tau}^\dagger\}$, where $\vec{r}$ is the position vector, σ the projection of the nucleon spin along the z axis, and τ its isospin projection.

A. Spectroscopic amplitudes

The physical processes providing information on the shell structure are one-nucleon transfer reactions. Although the discussion can be carried out for the transfer on any initial[2] many-body state, we restrict ourselves in the following to the transfer on the ground state $|\Psi_0^A\rangle$ of an even-even system, i.e. a $J^\pi = 0^+$ state. Furthermore, we consider this nucleus to be of *doubly closed-shell* character[3].

In this context, let us introduce U_μ (V_ν) as the amplitude to reach a specific eigenstate $|\Psi_\mu^{A+1}\rangle$ ($|\Psi_\nu^{A-1}\rangle$) of the A+1 (A-1) system by adding (removing) a nucleon in a specific single-particle state to (from) the ground state of the A-body system $|\Psi_0^A\rangle$. Such spectroscopic amplitudes can be defined through their representation in any given single-particle basis. In basis $\{a_p^\dagger\}$, they read

$$U_\mu^p \equiv \langle \Psi_\mu^{A+1}|a_p^\dagger|\Psi_0^A\rangle^* \ , \tag{2a}$$

$$V_\nu^p \equiv \langle \Psi_\nu^{A-1}|a_p|\Psi_0^A\rangle^* , \tag{2b}$$

whereas the representation in basis $\{b_{\vec{r}\sigma q}^\dagger\}$ provides the associated wave functions or *overlap functions*

$$U_\mu(\vec{r}\sigma\tau) \equiv \langle \Psi_\mu^{A+1}|b_{\vec{r}\sigma\tau}^\dagger|\Psi_0^A\rangle^* \ , \tag{3a}$$

$$V_\nu(\vec{r}\sigma\tau) \equiv \langle \Psi_\nu^{A-1}|b_{\vec{r}\sigma\tau}|\Psi_0^A\rangle^* . \tag{3b}$$

An important property regarding the asymptotic behaviour of overlap functions derives from their equation of motion given by [17]

$$[h^\infty + \Sigma(\omega)]_{\omega=E_\mu^+} U_\mu = E_\mu^+ U_\mu \ , \tag{4}$$

and similarly for (V_ν, E_ν^-), where (observable) one-nucleon separation energies are defined through

$$E_\mu^+ \equiv E_\mu^{A+1} - E_0^A \ , \tag{5a}$$

$$E_\nu^- \equiv E_0^A - E_\nu^{A-1} \ . \tag{5b}$$

The energy-*dependent* potential $\Sigma(\omega)$ denotes the *dynamical* part of the irreducible self-energy [17] that naturally arises in self-consistent Green's-function theory and that is evaluated at the eigensolution E_μ^+ in Eq. (4). The static field h^∞ is defined in Eq. (19) and contains both the kinetic energy and the energy-*independent* part of the self-energy. One can show from[4] Eq. (4) that the long-distance behaviour of the radial part of the overlap function is governed by the corresponding one-nucleon separation energy, e.g. for $E_\mu^+ < 0$

$$U_\mu(r\sigma\tau) \xrightarrow[r\to+\infty]{} A_\mu^+ \frac{e^{-\varsigma_\mu^+ r}}{\varsigma_\mu^+ r} \ , \tag{6}$$

where A_μ^+ denotes the so-called asymptotic normalization coefficient (ANC) while the decay constant is given by $\varsigma_\mu^+ \equiv (-2mE_\mu^+/\hbar^2)^{1/2}$, where m is the nucleon mass[5]. A similar result can, of course, be obtained for $V_\nu(r\sigma\tau)$ whose decay constant ς_ν^- relates to E_ν^-.

From spectroscopic amplitudes one defines addition S_μ^+ and removal S_ν^- spectroscopic probability matrices associated with states $|\Psi_\mu^{A+1}\rangle$ and $|\Psi_\nu^{A-1}\rangle$, respectively. Their matrix elements read in basis $\{a_p^\dagger\}$

$$S_\mu^{+pq} \equiv \langle \Psi_0^A|a_p|\Psi_\mu^{A+1}\rangle\langle \Psi_\mu^{A+1}|a_q^\dagger|\Psi_0^A\rangle \tag{7a}$$
$$= U_\mu^p U_\mu^{q*} \ ,$$

$$S_\nu^{-pq} \equiv \langle \Psi_0^A|a_q^\dagger|\Psi_\nu^{A-1}\rangle\langle \Psi_\nu^{A-1}|a_p|\Psi_0^A\rangle \tag{7b}$$
$$= V_\nu^{p*} V_\nu^q \ ,$$

such that their diagonal parts, when expressed in the coordinate space basis, are nothing but the *transition densities* for the one-nucleon transfer from $|\Psi_0^A\rangle$ to $|\Psi_\mu^{A+1}\rangle$ and $|\Psi_\nu^{A-1}\rangle$, respectively.

---

[2] There exists, in principle, as many different sets of ESPEs as there are eigenstates $|\Psi_\mu^A\rangle$ the one-nucleon transfer can be performed on [12].

[3] Note that such a notion can be misleading, especially in the context of the present discussion, as it relates to the filling of shells in the uncorrelated picture.

[4] This is obtained by expressing Eq. (4) in basis $\{b_{\vec{r}\sigma\tau}^\dagger\}$ and by using the short-range nature of nuclear forces to show that the non-local fields $h_{\vec{r}\sigma\tau \vec{r}'\sigma'\tau'}^\infty$ and $\Sigma_{\vec{r}\sigma\tau \vec{r}'\sigma'\tau'}(E_\mu^+)$ go to zero as $|\vec{r}'| \to +\infty$.

[5] Subtracting the center-of-mass motion would lead to using the reduced mass of the added/removed nucleon.

Tracing the two spectroscopic probability matrices over the one-body Hilbert space $\mathcal{H}_1$ gives access to spectroscopic *factors*

$$SF_\mu^+ \equiv \sum_{p \in \mathcal{H}_1} \left|U_\mu^p\right|^2 = \sum_{\sigma\tau} \int d\vec{r} \, |U_\mu(\vec{r}\sigma\tau)|^2 \, , \quad (8a)$$

$$SF_\nu^- \equiv \sum_{p \in \mathcal{H}_1} \left|V_\nu^p\right|^2 = \sum_{\sigma\tau} \int d\vec{r} \, |V_\nu(\vec{r}\sigma\tau)|^2 \, , \quad (8b)$$

which are nothing but the (basis-independent) norm of spectroscopic amplitudes. A spectroscopic factor characterizes to what extent an eigenstate of the A+1 (A-1) system can be described as a nucleon added to (removed from) a single-particle state on top of the ground-state of the A-nucleon system. Such a feature intrinsically depends on the resolution scale Λ characterizing the nuclear Hamiltonian and is thus not, strictly speaking, observable [18, 19]. Still, spectroscopic factors can serve as a tool to analyse the results obtained at a given resolution scale.

B. Spectral function and spectral strength distribution

We now gather the complete spectroscopic information associated with one-nucleon addition and removal processes in the so-called spectral function $\mathbf{S}(\omega) \equiv \mathbf{S}^+(\omega) + \mathbf{S}^-(\omega)$. The spectral function denotes an energy-*dependent* matrix over $\mathcal{H}_1$ whose elements in basis $\{a_p^\dagger\}$ are defined through

$$\mathbf{S}_{pq}(\omega) \equiv \sum_{\mu \in \mathcal{H}_{A+1}} S_\mu^{+pq} \, \delta(\omega - E_\mu^+) + \sum_{\nu \in \mathcal{H}_{A-1}} S_\nu^{-pq} \, \delta(\omega - E_\nu^-),$$

where the first (second) sum is restricted to eigenstates of H in the Hilbert space $\mathcal{H}_{A+1}$ ($\mathcal{H}_{A-1}$) associated with the A+1 (A-1) system. It is of interest to introduce the nth moment of the spectral function that defines an energy-*independent* matrix over $\mathcal{H}_1$ through

$$\mathbf{M}^{(n)} \equiv \int_{-\infty}^{+\infty} \omega^n \, \mathbf{S}(\omega) \, d\omega. \quad (9)$$

One can easily prove that the zeroth-moment is nothing but the identity matrix

$$\mathbf{M}_{pq}^{(0)} = \sum_{\mu \in \mathcal{H}_{A+1}} S_\mu^{+pq} + \sum_{\nu \in \mathcal{H}_{A-1}} S_\nu^{-pq} = \delta_{pq} \, , \quad (10)$$

such that the diagonal matrix element of $\mathbf{S}(\omega)$ possesses the meaning of a probability distribution function (PDF) in the statistical sense, i.e. the combined probability of adding and removing a nucleon to/from a specific single-particle basis state $|p\rangle$ integrates to 1 when summing over all final states in the A±1 systems.

Last, but not least, we introduce the spectral strength distribution (SDD) as the trace of the spectral function
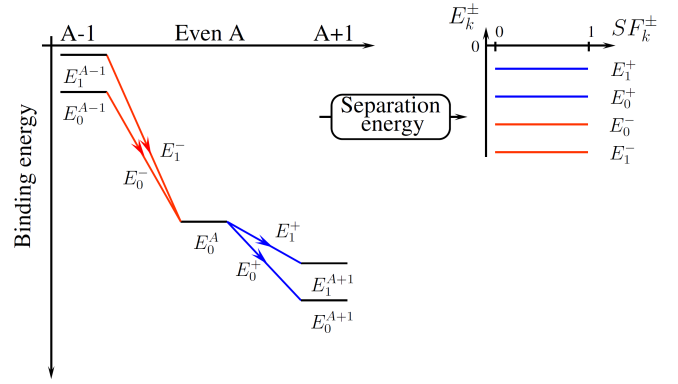

FIG. 1: (Color online) Schematic representation of one-nucleon addition and removal spectroscopic information for an independent-particle system. Left: binding energy for the ground-state of an even-even system and for the states of neighbouring nuclei reached by direct one-nucleon addition and removal processes. Right: corresponding spectral strength distribution.

matrix

$$\mathcal{S}(\omega) \equiv \text{Tr}_{\mathcal{H}_1} \left[\mathbf{S}(\omega)\right] \quad (11)$$
$$= \sum_{\mu \in \mathcal{H}_{A+1}} SF_\mu^+ \, \delta(\omega - E_\mu^+) + \sum_{\nu \in \mathcal{H}_{A-1}} SF_\nu^- \, \delta(\omega - E_\nu^-) \, ,$$

which is a basis-independent function of the energy.

C. Independent-particle vs correlated systems

It is of pedagogical interest to discuss the typical patterns displayed by the spectral strength distribution of both independent-particle and correlated systems. The goal of this exercise is to illustrate in what sense observable one-nucleon separation energies cannot be interpreted as single-particle energies as soon as correlations are present in the system.

Figure 1 provides a schematic display of one-nucleon addition and removal spectroscopic information for an independent-particle system. As many-body eigenstates of H take the form of Slater determinants in this case, there exists a particular single-particle basis of $\mathcal{H}_1$ in which addition and removal spectroscopic probability matrices read

$$S_\mu^{+pq} = \delta_{p\mu} \, \delta_{pq} \, \delta_{pa} \, , \quad (12a)$$
$$S_\nu^{-pq} = \delta_{p\nu} \, \delta_{pq} \, \delta_{pi} \, ,$$

where i and a characterize occupied ("hole") and unoccupied ("particle") states in the Slater determinant associated with the A-nucleon ground-state, respectively. Consequently, and as illustrated in Fig. 1, the many-body states reached by direct one-nucleon addition and removal processes are in one-to-one correspondence with
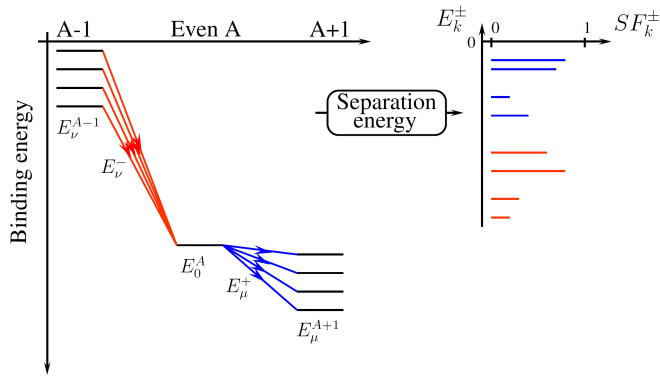
FIG. 2: (Color online) Same as Fig. 1 for a correlated system.

single-particle basis states. As a result of such a bijection, one-nucleon separation energies are good candidates to play the role of single-particle energies. As a matter of fact, one necessarily has $E_\mu^+ = \epsilon_a\,\delta_{a\mu}$ and $E_\nu^- = \epsilon_i\,\delta_{i\nu}$, where ϵ_a and ϵ_i denote eigenvalues of the one-body Hamiltonian governing the uncorrelated system associated with unoccupied and occupied single-particle states, respectively. Because the SDD integrates to the dimension of $\mathcal{H}_1$ by construction, spectroscopic factors of the corresponding states are equal to 1 whereas they are equal to zero for all the remaining states that are not reached by the direct one-nucleon transfer.

Let us now move to a correlated system. In *any* single-particle basis $\{a_p^\dagger\}$ of $\mathcal{H}_1$, S_μ^{+pq} (S_ν^{-pq}) is now different from zero for any combination[6] of μ, p and q (ν, p and q). Consequently, the SDD is fragmented as schematically displayed in Figure 2, i.e. a larger number of many-body states are reached through the direct addition and removal of a nucleon compared to the uncorrelated case[7]. Accordingly, and because the SDD still integrates to the dimension of $\mathcal{H}_1$ by construction (see Eq. (10)), spectroscopic factors are smaller than one. As a result, the number of peaks with non-zero strength in the SDD is greater than the dimension of $\mathcal{H}_1$, which forbids the establishment of a bijection between this set of peaks and any basis of $\mathcal{H}_1$. The impossibility to realize such a bijection constitutes the most direct and intuitive way to understand why observable one-nucleon separation energies cannot be rigorously associated with single-particle energies when correlations are present in the system, i.e. as soon as many-body eigenstates of H differ from Slater determinants.

D. Effective single-particle energies

The discussion provided above underlines the fact that a rigorous definition of ESPEs is yet to be provided in the realistic context of correlated many-nucleon systems. A key question is: how can one extract a single-particle shell structure that is in one-to-one correspondence with a basis of $\mathcal{H}_1$ and screens out, or at least averages out, the effect of many-body correlations in a systematic and consistent manner? ESPEs should of course reduce to being eigenvalues of the one-body Hamiltonian in the limit of an uncorrelated system.

Let us make the hypothesis that ideal one-nucleon pick-up and stripping reactions have been performed such that separation energies (E_μ^+, E_ν^-) and spectroscopic amplitudes (overlap functions) $(U_\mu(\vec{r}\sigma\tau), V_\nu(\vec{r}\sigma\tau))$ have been extracted consistently, i.e. in a way that is consistent with the chosen nuclear Hamiltonian $H(\Lambda)$ defined at a resolution scale Λ. In such a context, a meaningful definition of ESPEs does exist and goes back to French [10] and Baranger [11]. It involves the computation of the so-called centroid *matrix* which, in an arbitrary spherical basis of $\mathcal{H}_1$[8] $\{a_p^\dagger\}$, reads[9]

$$h_{pq}^{\rm cent} \equiv \sum_{\mu \in \mathcal{H}_{A+1}} S_\mu^{+pq} E_\mu^+ + \sum_{\mu \in \mathcal{H}_{A-1}} S_\mu^{-pq} E_\mu^- \ , \quad (13a)$$

and is nothing but the first moment of the spectral function matrix $\mathbf{M}^{(1)}$ (see Eq. 9). ESPEs and associated single-particle states are extracted, respectively, as eigenvalues and eigenvectors of $h^{\rm cent}$, i.e. by solving

$$h^{\rm cent}\,\psi_p^{\rm cent} = e_p^{\rm cent}\,\psi_p^{\rm cent} \ , \quad (14)$$

where the resulting spherical basis is denoted as $\{c_p^\dagger\}$. Written in that basis, centroid energies invoke diagonal spectroscopic probabilities[10]

$$e_p^{\rm cent} \equiv \sum_{\mu \in \mathcal{H}_{A+1}} S_\mu^{+pp} E_\mu^+ + \sum_{\mu \in \mathcal{H}_{A-1}} S_\mu^{-pp} E_\mu^- \ , \quad (15)$$

and acquire the meaning of an average of one-nucleon separation energies weighted by the probability to reach corresponding A+1 (A-1) eigenstates by adding (removing) a nucleon to (from) a single-particle state $\psi_p^{\rm cent}$.

---

[6] Except for selection rules dictated by symmetries that lead, according to Eq. (21), to $\pi_p = \pi_\mu$, $j_p = J_\mu$ and $\tau_p = T_\mu - T_0$.

[7] Of course, the dimension of $\mathcal{H}_{A+1}$ or $\mathcal{H}_{A-1}$ remains the same whether the system is correlated or not.

[8] In the hypothesis that spectroscopic amplitudes are extracted/computed in the coordinate space representation as $U_\mu(\vec{r}\sigma\tau)$ and $V_\mu(\vec{r}\sigma\tau)$, one would use them to define the centroid field in the coordinate basis, i.e one would compute $h_{\vec{r}\sigma\tau\,\vec{r}'\sigma'\tau'}^{\rm cent}$.

[9] If introduced in connection with the one-nucleon transfer on an initial state with $J \neq 0$, the definition of the centroid energy must include an additional sum over the magnetic quantum number m_p in order to generate a spherical shell structure.

[10] The definition of $e_p^{\rm cent}$ sometimes incorporates the denominator $\sum_\mu S_\mu^{+pp} + \sum_\mu S_\mu^{-pp}$ in Eq. (15) to compensate for the possibility that, e.g. experimentally, normalization condition 10 might not be exhausted.

Centroid energies are by construction in one-to-one correspondence with states of a single-particle basis of $\mathcal{H}_1$ which, as already pointed out before, is *not* the case of correlated one-nucleon separation energies with non-zero spectroscopic strength.

Equation (14) ensures that the asymptotic form of $\psi_p^{\mathrm{cent}}(\vec{r}\sigma\tau)$ is governed by the associated ESPE, e.g. for $e_p^{\mathrm{cent}} < 0$ the radial part of the wave function behaves asymptotically as

$$\psi_p^{\mathrm{cent}}(r\sigma\tau) \underset{r\to+\infty}{\longrightarrow} C_p \, \frac{e^{-\xi_p r}}{\xi_p \, r} \; , \tag{16}$$

where $\xi_p \equiv (-2m e_p^{\mathrm{cent}}/\hbar^2)^{1/2}$. Such a result underlines that single-particle wave-functions associated with ESPEs are intrinsically different from overlap functions $U_\mu(r\sigma\tau)$ $(V_\nu(r\sigma\tau))$ which are probed in transfer experiments. While the latter decay at long distances with physical, observable, separation energies E_μ^+ (E_ν^-), the asymptotic form of the former is governed by centroid energies e_p^{cent} associated with a given set of symmetry quantum numbers (Π_μ, J_μ, T_μ). The transformation taking care of such a change of asymptote reads

$$U_\mu(\vec{r}\sigma\tau) = \sum_{p\in\mathcal{H}_1} U_\mu^p \, \psi_p^{\mathrm{cent}}(\vec{r}\sigma\tau) \; , \tag{17a}$$

$$V_\mu(\vec{r}\sigma\tau) = \sum_{p\in\mathcal{H}_1} V_\mu^p \, \psi_p^{\mathrm{cent}\,*}(\vec{r}\sigma\tau) \; . \tag{17b}$$

E. Sum rule

It is tedious but straightforward to prove that the nth moment of $\mathbf{S}(\omega)$ fulfils the identity

$$\mathbf{M}_{pq}^{(n)} = \langle \Psi_0^{\mathrm{A}} | \{ \overbrace{[\dots[[a_p, H], H], \dots]}^{n\,\mathrm{commutators}}, a_q^\dagger \} | \Psi_0^{\mathrm{A}} \rangle . \tag{18}$$

Using the second quantized form of T, $V^{2\mathrm{N}}$, and $V^{3\mathrm{N}}$, together with identities provided in Appendix A and symmetries of the interaction matrix elements, Eq. (18) applied to $n = 1$ leads to [11, 12]

$$\begin{aligned} h_{pq}^{\mathrm{cent}} &= T_{pq} + \sum_{rs} \bar{V}_{prqs}^{2\mathrm{N}} \, \rho_{sr}^{[1]} + \frac{1}{4} \sum_{rstv} \bar{V}_{prtqsv}^{3\mathrm{N}} \, \rho_{svrt}^{[2]} \\ &\equiv h^\infty \; , \end{aligned} \tag{19}$$

where $\bar{V}_{prqs}^{2\mathrm{N}}$ and $\bar{V}_{prtqsv}^{3\mathrm{N}}$ are anti-symmetrized matrix elements and where

$$\rho_{pq}^{[1]} \equiv \langle \Psi_0^{\mathrm{A}} | a_q^\dagger a_p | \Psi_0^{\mathrm{A}} \rangle = \sum_\mu V_\mu^{p*} \, V_\mu^q \; , \tag{20a}$$

$$\rho_{pqrs}^{[2]} \equiv \langle \Psi_0^{\mathrm{A}} | a_r^\dagger a_s^\dagger a_q a_p | \Psi_0^{\mathrm{A}} \rangle \; , \tag{20b}$$

denote one- and two-body density matrices of the *correlated* A-body ground-state, respectively. The static field h^∞, already introduced in Sec. II A, contains both the

kinetic energy and the energy-*independent* part of the one-nucleon self-energy in the A-body ground state.

Equation (19) demonstrates that the centroid matrix is a one-body field possessing a simple structure and an intuitive meaning. In particular, the centroid field reduces to the Hartree-Fock (HF) mean field in the HF approximation. As a result, ESPEs are nothing but HF single-particle energies in such a case and are equal to one-nucleon separation energies according to Koopmans' theorem [20]. Consistently, overlap, centroid, and HF single-particle wave-functions coincide in that limit. Of course, centroid energies also reduce to eigenvalues of the one-body Hamiltonian in the limit of an uncorrelated system. When correlations beyond HF are switched on, ESPEs are modified through the presence of correlated density matrices in Eq. (19); i.e. the B-nucleon interaction is folded with the correlated (B-1)-body density matrix $\rho^{[\mathrm{B-1}]}$. Doing so, ESPEs continuously evolve as centroid energies rather than as observable separation energies such that the analogue of Koopmans' theorem does not hold any more. Centroid energies are schematically compared to observable binding and separation energies in Figure 3.

On the practical side, Eq. (19) underlines that the averaged information contained in ESPEs only requires the computation of the A-body ground-state. As long as one is not interested in the full spectroscopic strength of the A±1 systems but only in their centroids, one only needs to compute one nucleus instead of three.

F. Connection to monopole interaction

As mentioned above, many-body correlations are not entirely taken away from ESPEs. Still, most correlations are indeed screened out, which we now qualify in a different way, retaining 2N forces only for simplicity.

Working in basis $\{a_p^\dagger\}$, Wigner-Eckart's theorem allows one to obtain the explicit dependence of spectroscopic amplitudes on m_p and M_μ, i.e.

$$U_\mu^p \equiv U_{n_\mu}^{n_p\,[\alpha_p]} \, \delta_{\kappa_\mu\alpha_p} \, \delta_{M_\mu m_p} \; , \tag{21a}$$

$$V_\mu^p \equiv V_{n_\mu}^{n_p\,[\alpha_p]} \, \delta_{\kappa_\mu\alpha_p} \, \delta_{M_\mu - m_p} \, (-1)^{m_p}, \tag{21b}$$

such that the single-particle operator picks out the angular momentum, the parity and the isospin projection of the A±1 state the transfer goes to; i.e. $j_p = J_\mu$, $\pi_p = \Pi_\mu$ and $\tau_p = T_\mu - T_0$. Consequently, the one-body density matrix of the A-body ground state reads

$$\rho_{pq}^{[1]} \equiv \rho_{n_p n_q}^{[\alpha]} \, \delta_{\alpha_p \alpha_q} \, \delta_{m_p m_q} . \tag{22}$$

Expressing anti-symmetrized matrix elements in a jj-coupled scheme

$$\bar{V}_{pqrs}^{2\mathrm{N}} = \sum_{JMJ'M'} f_{\alpha_p\alpha_q\alpha_r\alpha_s}^{n_p n_q n_r n_s} C_{j_p m_p j_q m_q}^{JM} C_{j_r m_r j_s m_s}^{J'M'} \bar{V}_{n_p\alpha n_q\beta n_r\gamma n_s\delta}^{JMJ'M'},$$

where

$$f_{\alpha_p\alpha_q\alpha_r\alpha_s}^{n_p n_q n_r n_s} \equiv \sqrt{1 + \delta_{\alpha_p\alpha_q} \, \delta_{n_p n_q}} \sqrt{1 + \delta_{\alpha_r\alpha_s} \, \delta_{n_r n_s}} \; , \tag{23}$$
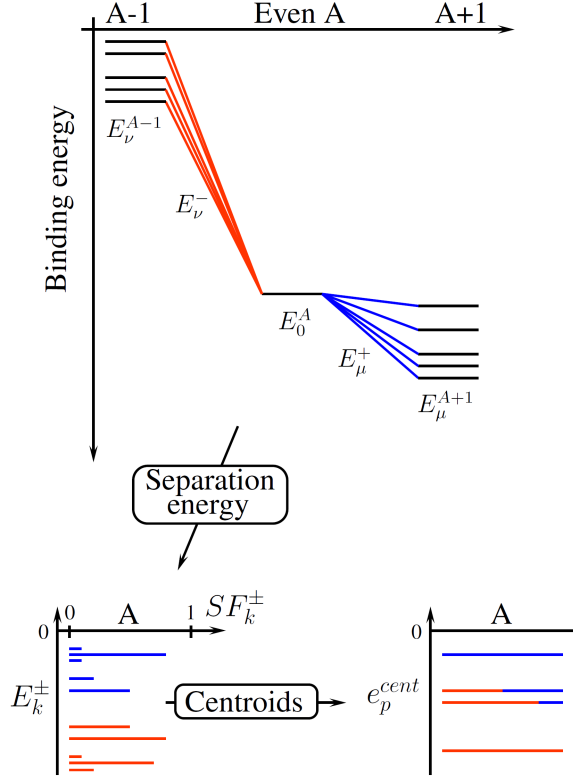
FIG. 3: (Color online) Schematic picture. Top: total binding energies (Eq. 1) of three successive nuclei and associated one-nucleon addition/removal energies (Eq. 5) from the ground state of the intermediate system. Bottom left: spectral strength distribution (Eq. 11) playing the role of a correlated "single-particle-like" spectrum. Bottom right: corresponding ESPE spectrum (Eq. 15). The color coding underlines that ESPEs close to the Fermi energy contain significant contributions from both addition and removal channels.

while $C^{JM}_{j_p m_p j_q m_q}$ denotes a Clebsch-Gordan coefficient and

$$\bar{V}^{JMJ'M'}_{n_p \alpha_p n_q \alpha_q n_r \alpha_r n_s \alpha_s} \equiv \delta_{JJ'} \, \delta_{MM'} \, \bar{V}^{J\,[\alpha_p \alpha_q \alpha_r \alpha_s]}_{n_p n_q n_r n_s} \,, \quad (24)$$

one obtains [11–13] in basis $\{c_p^\dagger\}$

$$e^{\text{cent}}_{n_p [\alpha_p]} = t^{[\alpha_p]}_{n_p n_p} + \sum_{n_q n_r} \sum_{\alpha_q} \bar{v}^{[\alpha_p \alpha_q \alpha_p \alpha_s]}_{n_p n_q n_p n_r} \, \rho^{[\alpha_q]}_{n_r n_q} \,, \quad (25)$$

where

$$\bar{v}^{[\alpha_p \alpha_q \alpha_p \alpha_q]}_{n_p n_q n_p n_r} \equiv \sum_J f^{n_p n_q n_p n_r}_{[\alpha_p \alpha_q \alpha_p \alpha_q]} \frac{2J+1}{2j_p+1} \bar{V}^{J\,[\alpha_p \alpha_q \alpha_p \alpha_q]}_{n_p n_q n_p n_r}$$

$$(26)$$

is the reduction of the 2N interaction to its so-called *monopole part*. Higher multipoles and in particular the quadrupole part that drives the dominant part of correlations are screened out from ESPEs.

G. Resolution-scale dependence

Let us briefly explain the intrinsic resolution-scale dependence of ESPEs. Such a feature derives directly from the resolution scale of spectroscopic amplitudes [18, 19] entering the definition of the centroid matrix, see Eq. (13a). Following the philosophy of the similarity renormalization group (SRG) [21, 22], we consider a change of resolution scale via a unitary transformation $U(\Lambda)$ of the Hamiltonian

$$H(\Lambda) \equiv U(\Lambda) \, H \, U^\dagger(\Lambda) \quad (27a)$$
$$\equiv T + V^{2\text{N}}(\Lambda) + V^{3\text{N}}(\Lambda) + \dots \,, \quad (27b)$$

where the scale characterizing the initial H is omitted for simplicity. As can be trivially shown, Eq. (27a) induces a transformation of eigenvectors of Eq. (1)

$$|\Psi^A_\mu(\Lambda)\rangle \equiv U^\dagger(\Lambda) \, |\Psi^A_\mu\rangle \,, \quad (28)$$

such that[11] the associated observable, i.e. the eigenenergy, remains unchanged $E^A_\mu(\Lambda) = E^A_\mu$. Similarly, any observable associated with a Hermitian operator O must remain invariant, which imposes the transformation of O according to $O(\Lambda) \equiv U(\Lambda) \, O \, U^\dagger(\Lambda)$.

Let us now come to ESPEs. The key difference from an observable resides in the fact that the very nature of ESPEs is to inform us of effective single-nucleon degrees of freedom inside the nuclear medium, independently of the form of the Hamiltonian. In other words, the *choice* is made to keep the definition of ESPEs independent of Λ. Before or after unitary transformation 27a, ESPEs are always extracted through Eq. (13a), where $S^{\pm\,pq}_\mu(\Lambda)$ retains the same formal expression as before, i.e. they invoke spectroscopic amplitudes computed through

$$U^p_\mu(\Lambda) \equiv \langle \Psi^{A+1}_\mu(\Lambda)|a_p^\dagger|\Psi^A_0(\Lambda)\rangle^* \,, \quad (29a)$$
$$V^p_\nu(\Lambda) \equiv \langle \Psi^{A-1}_\nu(\Lambda)|a_p|\Psi^A_0(\Lambda)\rangle^* \,. \quad (29b)$$

Contrary to the many-body states involved, operators $a_p^\dagger$ and a_p are *not* transformed in Eq. (29), which generates automatically an intrinsic dependence on Λ. One could, of course, choose to transform those operators in the definition of the spectroscopic amplitudes in order to make the latter invariant under the unitary transformation. However, transforming $a_p^\dagger$, e.g., would generate a linear combination of operators of the form $a_q^\dagger$, $a_q^\dagger a_r^\dagger a_s$, ... such that the spectroscopic amplitude would not provide the

---

[11] In practical applications, such an invariance is broken to some extent due to the approximate way of performing the transformation of the Hamiltonian, e.g. neglecting induced many-body interactions in Eq. (27b), and due to approximations performed when solving the A-body problem [23, 24]. However, the discussion of the present section is concerned with tracking what happens in the hypothesis of an exact unitary transformation and an exact solution of the A-body Schroedinger equation.

information one was after in the first place, e.g. access the overlap between eigenstates of $H(\Lambda)$ in the A+1 (A-1) system and the state obtained by adding (removing) a nucleon to (from) a given single-particle state $|p\rangle$ on top of the A-body ground-state. Eventually, the resolution-scale dependence of spectroscopic amplitudes propagates to their norm, i.e. spectroscopic factors [18, 19], and to ESPEs.

The discussion provided above points to an important conclusion. The information one is sometimes after, e.g. computing spectroscopic factors and ESPEs, is not necessarily an observable. Such information is not absolute and can be modified by a redefinition of inaccessible quantities, i.e. the Hamiltonian and its eigenvectors in the present case, which leaves true observables untouched. It remains to be seen how much ESPEs are changed in actual calculations by varying the resolution scale Λ on a reasonable interval of interest. This question is addressed in Sec. IV. It could very well be that the induced variation of the ESPEs is negligible compared to other sources of uncertainties, e.g. approximations in their computation. Still, it is of prime importance to keep such an intrinsic model dependence of ESPEs in mind.

H.   Remarks

Having summarized essentially known, though sometimes forgotten, results, we are now in the position of summarizing important points that will be referred to later on.

- A meaningful single-particle shell structure must fulfil a certain set of properties and known limits, i.e. only certain definitions are acceptable. Effective single-particle energies must (i) be independent of the particular single-particle basis one is working with and cannot be defined in an arbitrarily chosen basis, (ii) be computable using only quantities coming out of the correlated A-body Schrodinger equation, (iii) reduce to HF single-particle energies in the HF approximation to the A-body problem.

- There indeed exists, at least, one procedure to extract a shell structure that fulfils all above properties via centroids of correlated one-nucleon separation energies [10–12]. Thus defined, ESPEs are the eigenvalues of an effective one-body field h^{cent} that reduces to the HF one-body field within the HF approximation. Consequently, ESPEs evolve from being true separation energies within such an approximation (i.e. Koopmans' theorem) to being centroid energies when correlations are added beyond HF. Associated single-particle wave-functions change their meaning accordingly; i.e. while they match *overlap functions* decaying at long distances with observable separation energies in the uncorrelated limit, they do not play this role any more when correlations are added.

- Even when fulfilling the required set of minimal properties and known limits, ESPEs are not observable as they intrinsically depend on the resolution scale Λ characterizing the Hamiltonian, i.e. they change under a unitary transformation of the Hamiltonian that leaves true observables invariant. As such, they can only be used as an analysis tool for a fixed value of the resolution scale. Strictly speaking, no absolute statement can be made about the one-nucleon shell structure in a correlated spectrum; i.e. it is a scale-dependent concept.

- The computation of ESPEs requires the knowledge of one-body, two-body...density matrices of the *correlated* A-body state the one-nucleon transfer reaction is performed on, i.e. it is necessary to solve the *interacting* A-body problem to re-extract the shell structure. Although challenging, this constitutes a simplification compared to the necessity to solve the interacting problem for three successive nuclei when interested in the complete spectroscopic information. In practice however, Eq. (25) is rarely computed in terms of the correlated density matrix, e.g. shell-model applications usually invoke a filling approximation typical of an independent-particle approximation. This is believed to be a decent approximation as long as (i) low-lying states carry a major part of the single-particle spectroscopic strength, as for the transfer on a doubly closed-shell nucleus, and (ii) nucleons of the other species are themselves not strongly correlated, because of pairing for example. See, e.g., Ref. [25] and references therein for a related discussion. Such an issue becomes critical whenever one is looking into, e.g., the neutron shell structure of a neutron open-shell nucleus. In such a situation, a normal filling is inappropriate and it is mandatory to fold the monopole interaction in Eq. (25) with a density matrix reflecting the presence of correlations in the system.

- Theoretically, one can extract ESPEs either by performing the sum rule defined in Eq. (15) or by solving Eq. (14); see Ref. [25] for a comparative study within the frame of the nuclear shell model. Experimentally however, one can only perform the sum rule. Consequently, the extraction of reliable ESPEs requires, in principle, to collect the full spectroscopic strength, i.e. the complete set of separation energies and overlap functions from both one-nucleon stripping *and* pickup reactions. This unfortunately limits the possibility to perform sound comparisons on a systematic basis. Indeed, there are at best only a few nuclei along a given isotopic or isotonic chain that are characterized by complete enough spectroscopic data. Extraction from the data of reliable spectroscopic amplitudes in particular are difficult and usually rather model dependent. Contrary to what is sometimes stated, the

computation of ESPEs through Eq. (13a) requires the knowledge of spectroscopic *amplitudes*, or overlap functions, i.e. $U_\mu(\vec{r}\sigma\tau)$ and $V_\mu(\vec{r}\sigma\tau)$, and not only of associated spectroscopic factors, i.e. their norm. Doing so relies on a model that is most often empirical, e.g. modelling overlap functions as Woods-Saxon eigenfunctions whose asymptote is adjusted to fulfil Eq. (6). The dependence of the extracted information, e.g. spectroscopic factors, ANC and ESPEs, on the details of such a modelling remains as of today a source of rather uncontrolled uncertainty.

- In the definition used presently, which goes back to Ref. [11], ESPEs are univocally related to the one-body basis that diagonalizes the one-body field h^{cent}. The single-particle state ψ_p^{cent} and its associated ESPE e_p^{cent} are consistent in the sense that the asymptotic behaviour of the former is driven by the latter. Single-particle basis states ψ_p^{cent} naturally account for important physical features, such as polarization effects associated with the repeated addition of neutrons and protons to the system, as well as the impact of the virtual coupling to the one-body continuum when approaching the one-nucleon decay threshold. In practice however, the eigenbasis of h^{cent} is rarely used to compute ESPEs. In traditional shell-model applications for example, ESPEs are computed using harmonic oscillator wave-functions. This corresponds to defining e_p^{cent} as the diagonal matrix element h_{aa}^{cent}, where a denotes a harmonic oscillator state chosen a priori. Clearly, this leads to an inconsistency between the ESPE and its associated wave-function since the asymptotic of the latter does not reflect the former. How much such an inconsistency impacts the actual value of the ESPE thus calculated is a question that remains to be addressed systematically and quantitatively. This is relevant given the current bias towards studying the evolution of the nuclear shell structure as a function of N-Z and in the vicinity of the one-nucleon drip line.

III. COUPLED CLUSTER METHOD

One-nucleon separation energies and spectroscopic amplitudes introduced respectively in Eq. (5) and Eqs. (2-3) are defined without any reference to a particular method used to solve the many-body problem.

We are presently interested in using the ab-initio coupled-cluster method (CCM). Let us briefly outline the procedure to compute the ground and excited states of a closed (sub-)shell nucleus A and of the odd A±1 neighbours within CCM. From there, all needed quantities to compute ESPEs can be extracted. In CCM, the exact ground state is written in the exponential form

$$|\Psi_0^A\rangle = e^T|\Phi_0\rangle, \tag{30}$$

where $|\Phi_0\rangle$ is an uncorrelated single-reference Slater determinant built from a convenient spherical single-particle basis, usually chosen as mean-field HF orbitals. Many-body correlations beyond the mean field are introduced by the operator $T = T_1 + T_2 + \ldots + T_A$, which is a linear expansion in n-particle-n-hole excitation operators T_n, with $n = 1, \ldots, A$.

The only approximation occurring in CCM regards the truncation of T to a given low-lying excitation level; e.g. $T \approx T_1 + T_2$ is the most commonly used approximation known as the coupled-cluster method with single and double excitations (CCSD). Inserting the coupled-cluster ansatz (30) into the A-body Schrödinger equation (Eq. (1)) and projecting from the left with $\langle\Phi_0|e^{-T}, \langle\Phi_i^a|e^{-T}$ and $\langle\Phi_{ij}^{ab}|e^{-T}$ respectively, coupled-cluster equations are obtained under the form

$$\langle\Phi_0|e^{-T}He^T|\Phi_0\rangle = E_0^A, \tag{31a}$$

$$\langle\Phi_i^a|e^{-T}He^T|\Phi_0\rangle = 0, \tag{31b}$$

$$\langle\Phi_{ij}^{ab}|e^{-T}He^T|\Phi_0\rangle = 0. \tag{31c}$$

These equations determine the unknown amplitudes entering T_1 and T_2 as well as the ground state energy E_0^A. Here $\langle\Phi_i^a|$ and $\langle\Phi_{ij}^{ab}|$ are one-particle-one-hole and two-particle-two-hole excited reference states.

Equation (31) underlines that the similarity-transformed Hamiltonian $\bar{H} \equiv e^{-T}He^T$ plays a key role such that its ground state is nothing but the reference state $|\Phi_0\rangle$. The operator $\bar{H}$ is not Hermitian, which implies that coupled-cluster theory is manifestly non-variational. The non-variational nature of CCM makes it necessary to access both right *and* left eigenstates of $\bar{H}$ to compute associated one- and two-body density matrices. Such eigenstates of $\bar{H}$ can be computed through the so-called equation-of-motion coupled-cluster method (EOM-CCM). The idea of EOM-CC is essentially to diagonalize $\bar{H}$ within a subspace of n-particle-m-hole excited reference functions. Within the EOM-CCSD approximation, right and left eigenstates of closed-shell nucleus A are given by

$$|R_\mu^A\rangle = R_\mu^A|\Phi_0\rangle , \tag{32a}$$

$$\langle L_\mu^A| = \langle\Phi_0|L_\mu^A , \tag{32b}$$

where R_μ^A (L_μ^A) is a linear combination of one-particle-one-hole and two-particle-two-hole (de-)excitation operators. Similarly, EOM-CC is the method of choice to access eigenstates of odd A±1 neighbouring nuclei according to $|R_\mu^{A\pm1}\rangle = R_\mu^{A\pm1}|\Phi_0^A\rangle$ and $\langle L_\mu^{A\pm1}| = \langle\tilde{\Phi}_0^A|L_\mu^{A\pm1}$, where now $R_\mu^{A\pm1}$ ($L_\mu^{A\pm1}$) denotes a linear combination of one-particle (one-hole) and two-particle-one-hole (one-particle-two-hole) (de-)excitation operators (see for example Ref. [26] for further details). Left and right eigenstates form a bi-orthogonal set, i.e.

$$\langle L_\mu|R_{\mu'}\rangle = \delta_{\mu\mu'}. \tag{33}$$

where we have dropped the superscript referring to nucleus A and A±1. Right eigenstates R_μ are solutions of

the eigenvalue problem

$$(\bar{H}R_\mu)_C|\Phi_0\rangle = E_\mu R_\mu|\Phi_0\rangle \ , \qquad (34)$$

and similarly for left eigenstates L_μ. Here, $(\bar{H}R_\mu)_C$ denotes all terms that connect $\bar{H}$ with R_μ. The one- and two-body density matrices of the A-body ground state together with one-nucleon spectroscopic amplitudes and probabilities can now be computed according to

$$\rho^{[1]}_{pq} \equiv \langle\Phi_0|L_0^A \overline{a_q^\dagger a_p}|\Phi_0\rangle \ , \qquad (35a)$$

$$\rho^{[2]}_{pqrs} \equiv \langle\Phi_0|L_0^A \overline{a_r^\dagger a_s^\dagger a_q a_p}|\Phi_0\rangle \ , \qquad (35b)$$

and to

$$S^{+pq}_\mu \equiv \langle\Phi_0|L_0^A \overline{a_p} R_\mu^{A+1}|\Phi_0\rangle\langle\Phi_0|L_\mu^{A+1}\overline{a_q^\dagger}|\Phi_0\rangle \ , (36a)$$

$$S^{-pq}_\mu \equiv \langle\Phi_0|L_0^A \overline{a_q^\dagger} R_\mu^{A-1}|\Phi_0\rangle\langle\Phi_0|L_\mu^{A-1}\overline{a_p}|\Phi_0\rangle \ . (36b)$$

Using the Baker-Campbell-Hausdorff commutator expansion, one can derive finite and closed-form algebraic expressions for similarity-transformed operators $\overline{a_p}$, $\overline{a_p^\dagger}$, $\overline{a_q^\dagger a_p}$ and $\overline{a_r^\dagger a_s^\dagger a_q a_p}$[12].

IV. RESULTS

Results shown below have been obtained using a 2N force only, thereby omitting forces of higher rank. In order to improve convergence properties and make the nuclear many-body problem more perturbative, we use a soft $V_{\text{low-k}}$ 2N interaction [29] obtained with a smooth regulator [30] for various cutoff values between $\Lambda = 2.0\,\text{fm}^{-1}$ and $3.0\,\text{fm}^{-1}$. These soft $V_{\text{low-k}}$ interactions are obtained by evolving down the N^{3}LO Chiral interaction [31] with cutoff $\Lambda_\chi = 500\,\text{MeV}$. For the single-particle model space, we use the HF basis built from N+1= 13 major oscillator shells, with a fixed oscillator frequency of $\hbar\omega = 16\,\text{MeV}$. This model space is sufficient to obtain fully converged results for medium mass nuclei with soft $V_{\text{low-k}}$ interactions (see Ref.[16]).

A. Turning on correlations in a controlled way

Let us first illustrate in a pedagogical manner the effect of correlations on both one-nucleon separation energies and ESPEs. To do so, we apply Wick's theorem with respect to the HF vacuum $|\Phi_0^{\text{HF}}\rangle$ and write the Hamiltonian in normal-ordered form using the HF single-particle basis $\{d_p^\dagger\}$, i.e.
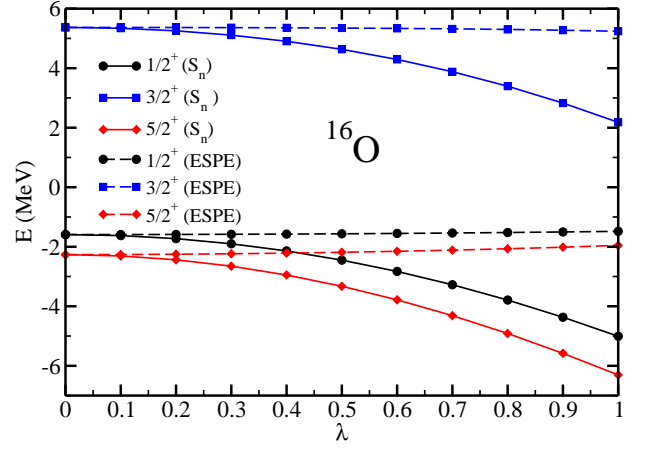
$$H = h^{\text{HF}} + V_{\text{res}} \ , \qquad (37)$$

---

[12] See Refs. [27, 28] for details on derivation and computation of spectroscopic factors within coupled-cluster theory.

FIG. 4: (Color online) One-neutron addition energies E_μ^+ on ^{16}O ground-state and corresponding ESPEs e_p^{cent} as a function of the residual interaction strength.

where

$$h^{\text{HF}} \equiv E_0^{\text{HF}} + \sum_p \epsilon_p^{\text{HF}} : d_p^\dagger d_p : \ , \qquad (38a)$$

$$V_{\text{res}} \equiv \frac{1}{4} \sum_{pqrs} \bar{V}^{2\text{N}}_{pqrs} : d_p^\dagger d_q^\dagger d_s d_r : \ , \qquad (38b)$$

together with

$$E_0^{\text{HF}} \equiv \sum_{p=1}^A T_{pp} + \frac{1}{2}\sum_{p,q=1}^A \bar{V}^{2\text{N}}_{pqpq} \ , \qquad (38c)$$

$$\epsilon_p^{\text{HF}} \equiv T_{pp} + \sum_{q=1}^A \bar{V}^{2\text{N}}_{pqpq} \ . \qquad (38d)$$

Scaling the residual interaction V_{res} by a factor $\lambda \in [0,1]$, one defines a parameter-dependent Hamiltonian $H_\lambda \equiv h^{\text{HF}} + \lambda V_{\text{res}}$ that tunes correlations between the two limits of interest, i.e. from the uncorrelated regime $H_0 = h^{\text{HF}}$ to the fully correlated regime $H_1 = H$. Eventually, we solve EOM-CC equations repeatedly for several values of $\lambda \in [0,1]$.

As a first example, Figure 4 displays, as a function of the residual interaction strength, one-neutron separation energies between ^{16}O ground-state and low-lying states in ^{17}O along with corresponding ESPEs. Plotted separation energies correspond to the (main) lowest peak in the additional sector of the SDD for each J^π symmetry block. As expected, one-neutron separation energies and ESPEs are equal in the uncorrelated limit ($\lambda = 0$) and are nothing but HF single-particle energies, i.e. Koopmans' theorem is fulfilled. Turning on correlations, two important features manifest themselves. First, the SDD is fragmented such that the separation energy of the state carrying the largest strength for a given J^π goes down significantly. Second, correlations only slightly impact centroid energies that keep a strong memory of HF single-particle energies. Thus, although ESPEs are
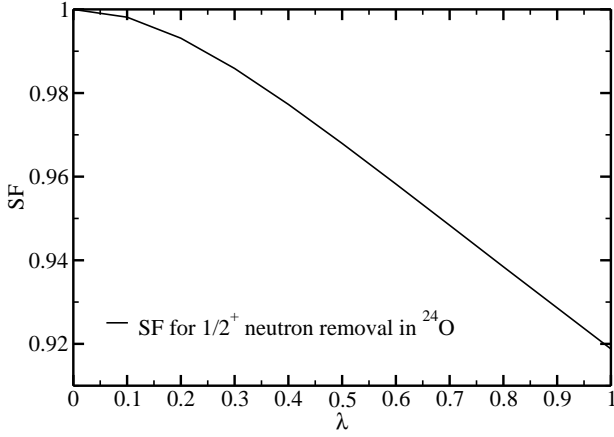
FIG. 5: (Color online) Removal spectroscopic factor $SF^-_{1/2^+}$ of the lowest $1/2^+$ state in ^{23}O as a function of the residual interaction strength.

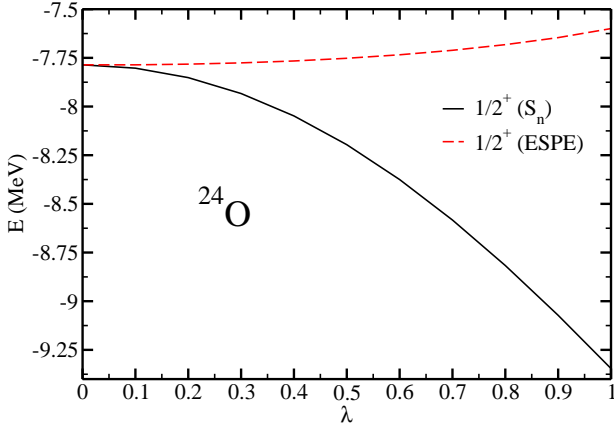FIG. 6: (Color online) Same as Figure 5 for one-neutron removal energy $E^-_{1/2^+}$ and ESPE $e^{\text{cent}}_{2s_{1/2}}$.

not independent of correlations, the latter are essentially screened out as discussed earlier. Eventually, one-nucleon separation energies and corresponding ESPEs can differ by several MeVs. This clearly points to the fact that separation energies should not be identified as ESPEs and vice versa.

Let us now include more detail by focusing on the lowest $1/2^+$ state in ^{23}O, which can be accessed by removing a neutron from the ground state of ^{24}O. Figure 5 displays the corresponding spectroscopic factor $SF^-_{1/2^+}$ as a function of the residual interaction strength. While $SF^-_{1/2^+} = 1$ for $\lambda = 0$ as expected, it decreases gently as the residual interaction is switched on to reach a value of 0.92 in the fully correlated case. Using it as a (scale-dependent) analysis tool, such a spectroscopic factor tells us that the lowest $1/2^+$ state displays a well-pronounced single-particle character even in the fully correlated limit.

Figure 6 shows the neutron separation energy and ESPE for that same $1/2^+$ state in ^{23}O as a function of λ. In the uncorrelated limit, i.e. $\lambda = 0$, the separa-
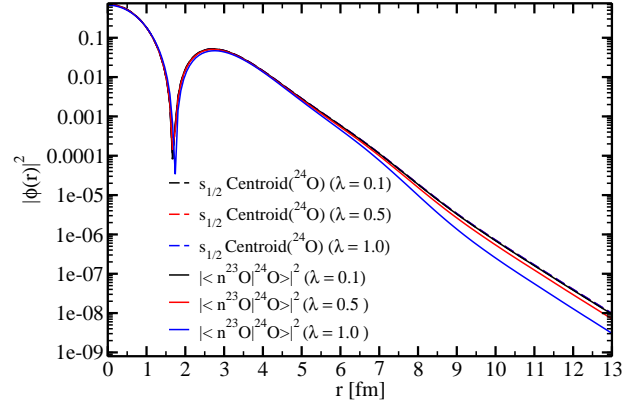

FIG. 7: (Color online) Square of neutron centroid wave-function $|\psi^{\text{cent}}_{2s_{1/2}}(r)|^2$ and overlap function $|V_{1/2^+}(r)|^2$ in ^{23}O for three values of the residual interaction strength. Centroid wave-functions are essentially on top of each others as their asymptotes are driven by ESPEs that are barely modified by switching on correlations.

tion energy and ESPE coincide, while for larger λ they start to deviate. While $e^{\text{cent}}_{2\,1/2^+}$ is only slightly influenced by correlations, $E^-_{1/2^+}$ dives significantly as λ increases from 0 to 1. Eventually, correlations add about 1.5 MeV to the separation energy, such that it differs from $e^{\text{cent}}_{2\,1/2^+}$ by 1.7 MeV for $\lambda = 1$. Consequently, even though the $1/2^+$ state retains to a large extent its single-particle nature, its energy is strongly impacted by correlations and does not provide clean information about the effective single-particle shell structure.

To complete the picture, Figure 7 compares the overlap function $|V_{1/2^+}(r)|^2$ of the $1/2^+$ state to the centroid wave-function $|\psi^{\text{cent}}_{2s_{1/2}}(r)|^2$, for three values of λ. In or-
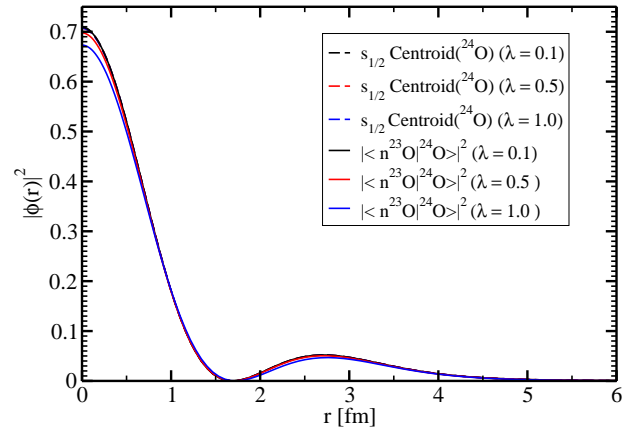

FIG. 8: (Color online) Same as Figure 7 but using a linear vertical scale.

der to ensure the correct exponential decay of the centroid and overlap functions, we used a Gamow HF basis built from 30 Woods-Saxon orbitals for the $s_{1/2}$ neutron partial-wave combined with $N + 1 = 13$ major oscilla-

tor shells for the remaining partial waves and protons. According to the previous discussion, as λ increases, the asymptotic form of the centroid wave-function remains unchanged while the exponential decay of the overlap function becomes faster from the increased separation energy. At the same time, Figure 8 provides a visual account of the fact that the norm of the overlap function slightly decreases with increasing λ, in agreement with Figure 5, while the centroid wave-function remains normalized by construction.

Last, but not least, Figure 9 compares, for $\lambda = 0.9$, the centroid wave-function $|\psi_{2s_{1/2}}^{cent}(r)|^2$ in ^{24}O to the asymptotic form (see Eq. (16)) computed from the corresponding centroid energy $e_{2s_{1/2}}^{cent} = -7.65$ MeV. The perfect agreement confirms the consistency between the ESPE and the single-particle wave-function it is computed from, which would not be the case if the former were computed from a harmonic oscillator state chosen a priori.
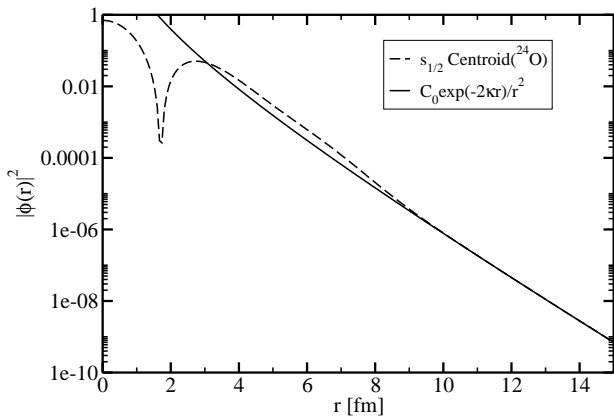

FIG. 9: (Color online) Square of the centroid wave-function $|\psi_{2s_{1/2}}^{cent}(r)|^2$ in ^{24}O for $\lambda = 0.9$ compared to the asymptotic form (see Eq. (16) computed from the corresponding centroid energy $e_{2s_{1/2}}^{cent} = -7.65$ MeV.

B. Systematics in oxygen and calcium isotopes

We now discuss the evolution and trends of low-lying one-neutron addition and removal energies together with centroid energies in doubly closed-shell oxygen and calcium isotopes. The present calculations are performed with the specific cutoff value $\Lambda = 2.4$ fm^{-1}. As a result, the neutron drip line in oxygen and calcium isotopes is wrongly predicted to be located beyond ^{28}O and ^{60}Ca, respectively. Three-body forces seem to be mandatory to correctly reproduce the drip line location at ^{24}O [4] for oxygen isotopes. It remains to be seen in which way forces of higher rank modify qualitatively or quantitatively the conclusions of the present investigation.

Figures 10 and 11 show that separation energies (E_μ^+, E_ν^-) systematically and significantly differ from corresponding centroid energies. As for the energetics, these
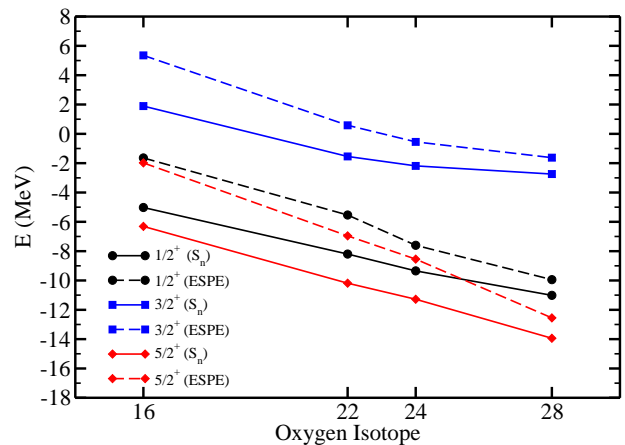

FIG. 10: (Color online) Evolution of selected one-neutron separation energies E_μ^+ and corresponding ESPEs e_p^{cent} from ^{16}O to ^{28}O.

results illustrate that ab-initio approaches describe doubly magic nuclei such as ^{16,24}O and ^{40,48}Ca as strongly correlated systems. Most importantly, how much separation energies differ from centroid energies significantly depends on the nucleus/state, in a way that cannot easily be traced back to one specific feature. Consequently, opening or closing of shell gaps in the separation energy spectrum are not in one-to-one relationship with those emerging in the ESPE spectrum. One does observe that ^{16}O and ^{40}Ca display the strongest correlations of all, which may be related to their N=Z character. Tracing the isospin dependence of correlations in oxygen and calcium isotopic chains, there seems to be a systematic trend with increasing asymmetry N-Z. In both oxygen and calcium chains, correlations become less important for the neutrons close to the Fermi surface when increasing isospin asymmetry N-Z. This trend is consistent with Ref. [32], where it was found that the spectroscopic factor for removing a neutron close to the Fermi surface increases with increasing isospin asymmetry and is close to one for ^{28}O, while the spectroscopic factor for removing the outermost protons is largely quenched with increasing isospin asymmetry.

As for the present study, the important point is to demonstrate that inferring one-nucleon separation energies from ESPEs is not straightforward, even in doubly closed-shell nuclei. Consequently, ESPEs must be used with care.

C. Effective shell model

Equation 19 was obtained following an ab-initio strategy, i.e. considering all nucleons as active and interacting via realistic 2N and 3N interactions appropriate to low-energy nuclear physics. A large enough single-particle Hilbert space was implied that ensures numerical convergence. In the traditional effective shell-model, how-
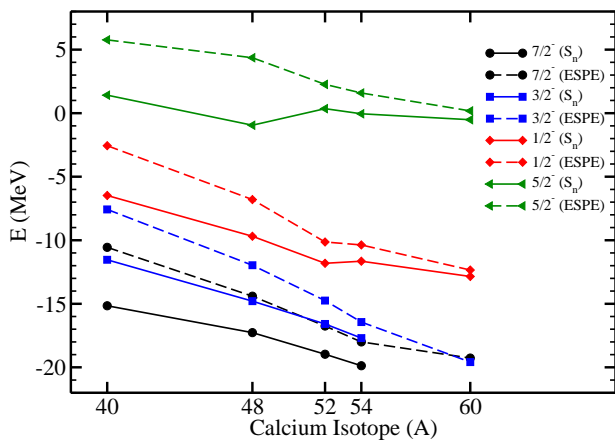
FIG. 11: (Color online) Same as Figure 10 from ^{40}Ca to ^{60}Ca.

ever, the equivalent of Eq. (19) is derived from an effective Hamiltonian defined for n^{val} active nucleons in a restricted valence space above a closed core composed of n^{core} nucleons and below an excluded space. One thus defines $H^{\text{eff}} \equiv h^{\text{core}} + V^{\text{val}}$ with $h_{pq}^{\text{core}} = e_p^{\text{core}} \delta_{pq}$, such that, in principle, solving the n^{val}-body problem in terms of H^{eff} provides exact energy eigenvalues for a set of nuclei heavier than the core. In such a context, ESPEs are "anchored" on (experimental) one-nucleon addition energies to the core nucleus, i.e. $e_p^{\text{core}} \equiv E_\mu^+ \delta_{pk}$. Considering more than one nucleon outside the core, the valence interaction effectively accounts for processes outside the valence space and ESPEs are computed via an adaptation of Eq. (19), i.e.

$$\epsilon_p^{\text{cent}} = e_p^{\text{core}} + \sum_{qr \in \text{val}} \bar{V}_{pqpr}^{\text{val}} \rho_{rq}^{\text{val}} , \qquad (39)$$

which involves the *valence space* correlated one-body density matrix ρ^{val} and the monopole part of the effective interaction.

As seen in previous sections, equating an observable separation energy $E_\mu^\pm$ with an ESPE e_p^{cent} is a bad approximation in doubly closed shell nuclei (± 1 nucleon) when taking an ab-initio perspective. However, and as confirmed by the present investigation, low-lying states obtained by adding (removing) one nucleon to (from) a doubly closed shell nucleus do possess a well-defined single-particle character. The reason why the corresponding ESPE differs significantly from the separation energy is due to the fact that the former collects small strength rejected to rather high missing energies. Eventually, the fact that low-lying states carry most of the strength makes them good candidates to represent *quasi* single-particle degrees of freedom. Such a textbook result constitutes the basic justification for the effective shell model that omits the high-lying fragmented strength and recollects the full strength into low-lying states of the core+one-nucleon system, i.e. postulating $e_p^{\text{core}} \equiv E_\mu^+ \delta_{pk}$. As long as the active valence space is large enough, such an approximation is amenable to the description of low-energy properties of nuclei above the closed-shell core.

D. Using a fixed single-particle basis

Computing ESPEs in an approximate fashion generates a model dependence that may compromise their usefulness. It is, for example, customary to use uncorrelated occupations of single-particle states in place of the correlated one-body density matrix in Eq. (19) and/or to define ESPEs as the diagonal matrix elements of the centroid field h^{cent} in an a priori chosen single-particle basis, e.g. a harmonic oscillator basis, rather than as its eigenvalues. The latter approximation is formally questionable as it provides a basis-dependent definition of ESPEs, the quality of which depends on the realistic character of the chosen basis. In practice, the quantitative impact of such an approximate scheme depends on the situation.

Figure 12 compares in oxygen isotopes properly computed ESPEs with diagonal matrix elements of h^{cent} in the HF basis used in the calculation[13]. As can be inferred from the comparison with Fig. 10, the approximation induces errors on ESPEs that are of the same order as their difference with one-nucleon separation energies and that are, in some cases, significant relative to their absolute values. The error depends both on the state and on the system, i.e. it might go in opposite directions depending on the state and/or the nucleus under consideration.

Interestingly, there exists cases for which the ordering of approximate ESPEs at the Fermi level is inverted compared to full-fledged ones, e.g. $2s_{1/2}$ and $1d_{5/2}$ levels in ^{22}O. Knowing that full-blown ESPEs reproduce the ordering of one-neutron separation energies across the whole set of oxygen and calcium isotopes, such an inversion is of noticeable importance. The inversion seen in ^{22}O is consistent with Fig. 2a of Ref. [4] where ESPEs were computed, as is customary within the frame of the interacting shell model, diagonal matrix elements of h^{cent} in an a priori chosen harmonic oscillator basis. The fact that $2s_{1/2}$ and $1d_{5/2}$ levels are actually not inverted in Fig. 2a of Ref. [4] is simply due to the fact that ESPEs are anchored on *empirical* values in ^{17}O. Correcting mentally for such a fact, one recovers the level inversion seen for "Diag-ESPE" in Fig. 12 of the present paper.

E. Resolution scale dependence

A more fundamental model dependence of ESPEs that remains even when computing them as eigenvalues of the

---

[13] A more drastic approximation not shown here consists in using diagonal matrix elements in a harmonic oscillator basis. This is the choice usually made within the frame of the interacting shell model.
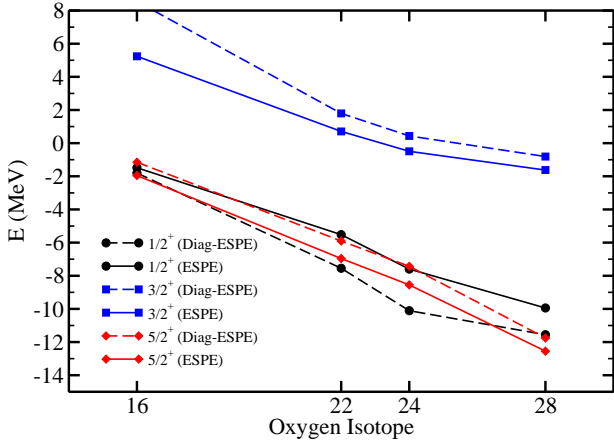
FIG. 12: (Color online) ESPEs $e_p^{\rm cent}$ compared to diagonal matrix elements of the centroid field $h_{qq}^{\rm cent}$ in the underlying HF basis. Results are displayed from ^{16}O to ^{28}O.

FIG. 13: (Color online) Neutron ESPEs and removal energies in ^{24}O for $J^\pi = 1/2^+, 5/2^+$ and $\Lambda \in [2.0, 3.0]$ fm^{-1}.

centroid matrix relates to the resolution scale characterizing the Hamiltonian. We start from a Chiral Hamiltonian built with a cutoff Λ_χ (e.g. 500 MeV here) up to a given order (e.g. N^{3}LO here). This in itself carries a truncation error with respect to using the complete EFT Lagrangian. This however constitutes our reference Hamiltonian, which at N^{3}LO contains both 2N and 3N interactions. In a second step, the resolution scale of the Hamiltonian is lowered to a value Λ through a renormalization group transformation, defining in this way $H(\Lambda) \equiv H_{\rm low-k}$. Doing so softens the interactions and induces multi-body forces, e.g. 3N interactions are induced from the original 2N one, while preserving the original truncation error. As Λ is lowered, true observables remain the same as with the original Chiral Hamiltonian as long as induced interactions are kept in the calculation and the many-body problem is solved exactly. Contrarily, even in such conditions non-observables quantities such as ESPEs are modified when changing Λ. This constitutes the *intrinsic* scale dependence of ESPEs discussed in Sec. II G and that we presently wish to characterize. Of course, in case induced interactions are discarded and/or the many-problem is not solved exactly, both observable and non-observable quantities acquire an additional *artificial*[14] dependence on Λ.

As original and induced three-body forces, as well as clusters beyond singles and doubles, are discarded in the present calculation, ESPEs display the two sources of Λ dependence. In order to extract the intrinsic one, one must first pin down the artificial scale dependence to subtract it eventually. By definition, the latter can be accessed by focusing on true observables. Figure 13 displays
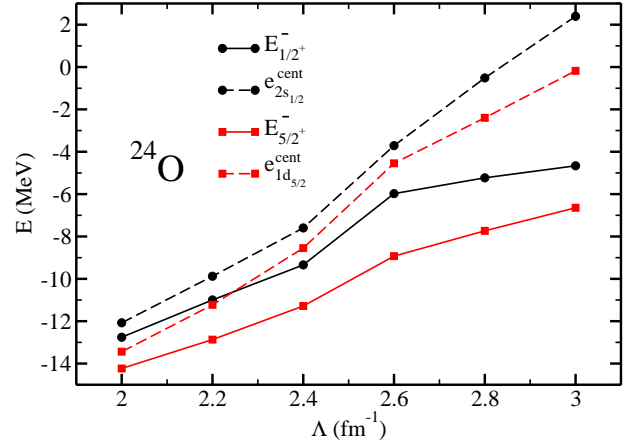
one-neutron removal energies with $J^\pi = 1/2^+, 5/2^+$ in ^{24}O for various values[15] of the momentum cutoff Λ of the 2N interaction $V_{\rm low-k}$. Lowering Λ from 3.0 to 2.0 fm^{-1} changes one-neutron removal energies by about 8 MeV. Eventually, including induced many-body interactions, i.e. three- and possibly four-body forces [23, 24], will remove such an artificial dependence of one-neutron removal energies on Λ.

Figure 13 also shows ESPEs $e_{2s_{1/2}}^{\rm cent}$ and $e_{1d_{5/2}}^{\rm cent}$ in ^{24}O. Clearly, they display a significantly larger cutoff variation than corresponding one-neutron removal energies. Such a feature, visible in all isotopes and for all states, is identified with the additional intrinsic scale dependence of ESPEs. Mentally subtracting the cutoff dependence of one-neutron removal energies, one sees that such an intrinsic scale dependence increases with Λ as the system becomes less and less perturbative, making ESPEs differ more and more from separation energies. Quantitatively speaking, the intrinsic cutoff dependence of $e_{2s_{1/2}}^{\rm cent}$ and $e_{1d_{5/2}}^{\rm cent}$ amounts to about 6 MeV when varying Λ from 2.0 to 3.0 fm^{-1}, which is obviously significant. More specifically, one notes that both ESPEs do not vary identically across the range of Λ values. Besides removing (most of) their artificial cutoff dependence, it will be of interest to see how much 3N forces modify the intrinsic scale dependence of ESPEs. It is anyway likely that the latter will remain significant.

The above result demonstrates that ESPEs are not absolute and can be changed significantly by modifying

---

[14] By *artificial* we mean a dependence introduced by compromising the unitarity of the renormalization group transformation and/or by solving the many-problem incompletely.

[15] We keep the oscillator frequency fixed at $\hbar\omega = 16$ MeV in present calculations. For large cutoff values, the optimal oscillator frequency is larger, e.g. $\hbar\omega = 24$ MeV for $\Lambda = 2.6$ fm^{-1}, such that corresponding values shown in Fig. 13 are not fully converged, e.g. they changed by about 100 keV for $\Lambda = 2.6$ fm^{-1} when using $\hbar\omega = 24$ MeV. Conclusions of the present section will however not be modified by using fully converged values.

mildly the character of the Hamiltonian, i.e. by varying Λ over a rather limited range of values. Consequently, extracting *the* single-particle shell structure and its evolution, e.g. with isospin, from experimental data is an illusory objective. Of course, it remains possible to perform a consistent analysis of experimental data at the price of working throughout the analysis with a fixed Hamiltonian characterized by a given resolution scale Λ. Still, conclusions regarding the extracted shell structure, i.e. its evolution with isospin, are necessarily be resolution-scale dependent.

F. Link between ESPE and $E_{2_1^+}$

Conventionally, a large shell gap in the ESPE spectrum is seen as the precursor of a high 2_1^+ excitation energy, and thus as the signature of a magic number. In order to test this "common knowledge", it is of interest to quantify how much $E_{2_1^+}$ does indeed correlate with the size of the gap at the Fermi energy in the ESPE spectrum, which we denote here as $\Delta e_{\rm F}^{\rm ESPE}$. Similarly, one may wonder how much $E_{2_1^+}$ correlates with the size of the gap at the Fermi energy in the observable one-nucleon separation energy spectrum. The latter is nothing but the difference between one-nucleon addition and removal energies associated with the ground state of the A+1 and A-1 systems, i.e. $E_0^+ - E_0^-$.

First, we compute the three quantities of interest in ^{22,24}O and ^{48,52}Ca for $\Lambda = 2.4$ fm^{-1}. The 2_1^+ excitation energy is obtained by solving the EOM-CCSD equations for excited states given in Eq. (34). The EOM-CCSD approach to excited states typically works well for states possessing a dominant $1p$-$1h$ structure. The 2_1^+ excited state in ^{16}O and ^{40}Ca being dominated by collective excitations, and having a very small $1p$-$1h$ component, are excluded from the present analysis. On the contrary, 2_1^+ states in ^{22,24}O and ^{48,52}Ca have a large $1p$-$1h$ component ($\sim 80\%$) and are well described through the EOM-CCSD approach. Such 2_1^+ states constitute the best case scenario as far as the present study is concerned, i.e. by definition their excitation energy is likely to correlate with the size of the gap in the ESPE spectrum.

The results are reported in Table I where the shell gap $\Delta e_{\rm F}^{\rm Diag-ESPE}$ obtained from ESPEs computed as diagonal matrix elements of the centroid field in the HF basis also appears in the last column. It is seen that the size of the gap at the Fermi energy is of the order of $E_{2_1^+}$ for both ESPE and one-nucleon separation energy spectra in the selected doubly closed shell nuclei. Focusing on ^{24}O and ^{52}Ca, one could be tempted to conclude similarly for $\Delta e_{\rm F}^{\rm Diag-ESPE}$. This is however invalidated by the results obtained for ^{22}O and ^{48}Ca due to the inversion of levels discussed in Sec. IV D that is signalled by a negative value of the gap in the last column of Table I.

In order to perform a more systematic analysis, calculations were repeated for several values of the low-

	$E_{2_1^+}$	$E_0^+ - E_0^-$	$\Delta e_{\rm F}^{\rm ESPE}$	$\Delta e_{\rm F}^{\rm Diag-ESPE}$
^{22}O	1.826	1.989	1.437	-1.536
^{24}O	7.477	7.176	7.104	8.715
^{48}Ca	2.388	2.475	2.435	-4.141
^{52}Ca	5.130	4.777	4.609	4.243

TABLE I: Excitation energy of the 2_1^+ state in selected oxygen and calcium isotopes along with the size of the gap at the Fermi energy in corresponding ESPE and one-nucleon separation energy spectra. A low-momentum interaction with a cutoff $\Lambda = 2.4$ fm^{-1} is used.
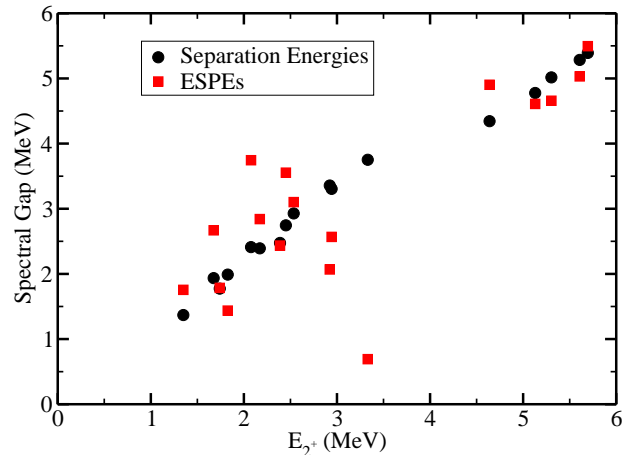

FIG. 14: (Color online) Separation-energy and ESPE gaps versus 2_1^+ excitation energy in ^{22}O and ^{48,52}Ca for $\Lambda \in [2.0, 3.0]$ fm^{-1}.

momentum cutoff Λ between 2.0 and 3.0 fm^{-1} in ^{22}O and ^{48,52}Ca. Due to the omission of 3N forces, values are unrealistic for most cases. This is not a concern given that we are presently interested in the way theoretical quantities correlate, independently of whether they account well for experimental data. Still, we exclude ^{24}O as the corresponding 2_1^+ excitation energy is unacceptably large in the present calculation. As seen in Fig. 14, a strong linear correlation arises between $E_{2_1^+}$ and the separation energy gap. On the other hand, the correlation with the ESPE gap is now far less substantial. As a matter of fact, the Pearson correlation coefficient quantifying the strength of the linear correlation between two variables is equal to 0.99 for the separation-energy gap and to 0.78 for the ESPE gap. Although such numbers are to be taken with a grain of salt given the small sample used in the present analysis, they reflect the different character of the correlation in both cases.

Even though the result obtained here calls for a more systematic study based on a statistically meaningful sample, it manifestly illustrates the fact that inferring the structure of a nucleus, e.g. its magic character, on the sole basis of the ESPE spectrum is questionable and should be avoided. For example, several data points shown in Fig. 14 contradict the "common knowledge"

that a large (small) $E_{2_1^+}$ necessarily relates to a large (small) gap at the Fermi energy in the ESPE spectrum. Indeed, no strict causal relationships exists between the two quantities. Although it will not come as a surprise for, e.g., shell model practitioners that the structure of certain nuclei is dominated by correlation effects beyond monopoles, it is not usually appreciated that correlations can effectively *enhance* the magic character of a nucleus by generating a large $E_{2_1^+}$ on top of a small gap in the ESPE spectrum. This is the case in ^{48}Ca for $\Lambda \in [2.4 - 2.8]$ fm^{-1}, which is consistent with the results obtained in (Figs. 1d and 2d of) Ref. [8] where the important role played by 3N interactions is highlighted.

V. CONCLUSIONS

The present work discusses, from an ab-initio standpoint, the definition, the meaning, and the usefulness of ESPEs in doubly closed shell medium-mass nuclei. Illustrating the various points with state-of-the-art coupled-cluster calculations, the following conclusions are reached.

- A meaningful single-particle shell structure fulfilling a minimal set of properties and known limits, such as being independent of the particular single-particle basis one is working with, can be extracted from correlated one-nucleon separation energies and associated spectroscopic amplitudes. Such a definition relates effective single-particle energies (ESPEs) to the so-called centroid eigenvalues introduced by Baranger [11].

- The corresponding non-interacting problem is governed by the one-body centroid field $h^{\rm cent}$, which is nothing but the *energy-independent* part of the one-nucleon self-energy that naturally appears in self-consistent Green's-function methods.

- It is customary in low-energy nuclear theory to compute ESPEs in an approximate fashion, e.g. by defining them as diagonal matrix elements of $h^{\rm cent}$ in an a priori chosen single-particle basis rather than as its eigenvalues. We have illustrated the fact that such approximations are unsafe.

- Extracting an effective shell structure, i.e. an effective single-particle picture, is often done for interpretation purposes and sometimes done to infer the behaviour of actual observables that are believed to be strongly correlated to patterns in the ESPE spectrum. Focusing on one-nucleon separation energies and the excitation energy of the first 2^+ state, we illustrate that

  1. One-nucleon separation energies of low-lying states are strongly impacted by correlations, even in good closed-shell nuclei, and do not provide direct information about the underlying effective single-particle shell structure. This is true even for states that retain a strong single-particle character, i.e. states carrying spectroscopic factors close to one.

  2. While the excitation energy of the first 2^+ state strongly correlates with the size of the gap at the Fermi energy in the observable one-nucleon separation energy spectrum, it is not the case for the gap in the ESPE spectrum. Such a result leads to the conclusion that inferring the structure of a nucleus, e.g. its magic character, on the sole basis of the ESPE spectrum is questionable and should be avoided.

- Even when fulfilling the required set of minimal properties, ESPEs are not strictly observable as they are intrinsically dependent on the resolution scale Λ of the Hamiltonian, i.e. they change under a unitary transformation of the Hamiltonian while true observables remain invariant. We have indeed demonstrated that ESPEs vary substantially when modifying mildly the resolution scale, i.e. when scanning a rather limited range of Λ values while correcting for the artificial dependence due to the omission of induced sort-range many-forces. Such a result demonstrates that the objective of extracting a *unique* single-nucleon shell structure from correlated observables, e.g. pinning down *the* nuclear shell evolution from experimental data, is intrinsically illusory. Still, it is possible to perform a consistent analysis of experimental data and extract a meaningful shell structure at the price of working throughout the analysis with a fixed Hamiltonian characterized by a given resolution scale Λ. Still, conclusions regarding the nuclear shell structure, i.e. its evolution with isospin, are scale dependent by definition.

- The present study was conducted on the basis of two-nucleon interactions only. It remains to be seen to which extent forces of higher rank modify our conclusions. At the price of computing ESPEs correctly, i.e. as eigenvalues of the centroid matrix rather thanas its diagonal matrix elements in an a priori given (harmonic oscillator) basis, the authors of Refs. [4, 8] could easily repeat the present analysis within the frame of the shell model and characterize the impact of three-nucleon forces in a systematic way.

- In the present work, ESPEs were defined based on the hypothesis that eigenstates of the nuclear Hamiltonian are also eigenstates of the particle number operator. Ab-initio calculations of open-shell nuclei are currently being developed on the basis of many-body methods breaking particle-number good symmetry, i.e. using methods for-

mulated over the Fock space rather than over the Hilbert space associated with a definite number of particles. This is the case of the so-called self-consistent Gorkov-Green's function theory [33]. Extending the definition of ESPEs accordingly [33], one should be able to address properties of ESPEs in open-shell nuclei and conclude on their relevance in such a context.

Acknowledgments

Appendix A: Useful identities

Using Wick's theorem, one can demonstrate the following identities

$$
\begin{aligned}
\{[a_p, a_r^\dagger a_s], a_q^\dagger\} &= +\delta_{pr}\,\delta_{qs} \ , \\
\{[a_p, a_r^\dagger a_s^\dagger a_t a_v], a_q^\dagger\} &= +\delta_{pr}\,\delta_{qv}\,a_s^\dagger a_t - \delta_{pr}\,\delta_{qt}\,a_s^\dagger a_v \\
&\quad -\delta_{ps}\,\delta_{qv}\,a_r^\dagger a_t + \delta_{ps}\,\delta_{qt}\,a_r^\dagger a_v \ , \\
\{[a_p, a_r^\dagger a_s^\dagger a_t^\dagger a_w a_v a_u], a_q^\dagger\} &= +\delta_{pr}\,\delta_{qu}\,a_s^\dagger a_t^\dagger a_w a_v - \delta_{pr}\,\delta_{qv}\,a_s^\dagger a_t^\dagger a_w a_u + \delta_{pr}\,\delta_{qw}\,a_s^\dagger a_t^\dagger a_v a_u \\
&\quad -\delta_{ps}\,\delta_{qu}\,a_r^\dagger a_t^\dagger a_w a_v + \delta_{ps}\,\delta_{qv}\,a_r^\dagger a_t^\dagger a_w a_u - \delta_{ps}\,\delta_{qw}\,a_r^\dagger a_t^\dagger a_v a_u \\
&\quad +\delta_{pt}\,\delta_{qu}\,a_r^\dagger a_s^\dagger a_w a_v - \delta_{pt}\,\delta_{qv}\,a_r^\dagger a_s^\dagger a_w a_u + \delta_{pt}\,\delta_{qw}\,a_r^\dagger a_s^\dagger a_v a_u \ .
\end{aligned}
$$

[1] M. Goeppert-Mayer, Phys. Rev. **75**, 1969 (1949).
[2] T. Baumann, A. M. Amthor, D. Bazin, B. A. Brown, C. M. Folden, A. Gade, T. N. Ginter, M. Hausmann, M. Mato, D. J. Morrissey, et al., Nature **449**, 1022 (2007).
[3] R. V. F. Janssens, Nature **459**, 1069 (2009).
[4] T. Otsuka, T. Suzuki, J. D. Holt, A. Schwenk, and Y. Akaishi, Phys. Rev. Lett. **105**, 032501 (2010).
[5] K. Tsukiyama, M. Hjorth-Jensen, and G. Hagen, Phys.Rev. **C80**, 051301 (2009).
[6] N. Michel, W. Nazarewicz, J. Okolowicz, and M. Ploszajczak, J.Phys.G **G37**, 064042 (2010).
[7] K. Tsukiyama, T. Otsuka, and R. Fujimoto (2010), 1001.0729.
[8] J. D. Holt, T. Otsuka, A. Schwenk, and T. Suzuki (2010), 1009.5984.
[9] J. Holt and A. Schwenk (2011), 1108.2680.
[10] J. B. French, in *Proceedings of the International school of physics Enrico Fermi, Varenna 1965*, edited by C. Bloch (Academic Press, New York, 1966), p. course 36.
[11] M. Baranger, Nucl. Phys. **A149**, 225 (1970).
[12] A. Umeya and K. Muto, Phys. Rev. **C74**, 034330 (2006).
[13] M. Dufour and A. Zuker, Phys. Rev. **C54**, 1641 (1996).
[14] R. K. Bansal and J. B. French, Phys. Lett. **11**, 145 (1964).
[15] A. Zuker, Phys. Rev. Lett. **23**, 983 (1969).
[16] G. Hagen, T. Papenbrock, D. J. Dean, and M. Hjorth-Jensen, Phys. Rev. **C82**, 034330 (2010).
[17] W. H. Dickhoff and C. Barbieri, Prog. Part. Nucl. Phys. **52**, 377 (2004).
[18] R. J. Furnstahl and H. W. Hammer, Phys. Lett. **B531**, 203 (2002).
[19] B. K. Jennings (2011), 1102.3721.
[20] T. H. Koopmans, Physica **1**, 104 (1934).
[21] S. K. Bogner, R. J. Furnstahl, and R. J. Perry, Phys. Rev. **C75**, 061001 (2007).
[22] E. R. Anderson, S. K. Bogner, R. J. Furnstahl, and R. J. Perry, Phys. Rev. **C82**, 054001 (2010).
[23] E. D. Jurgenson, P. Navratil, and R. J. Furnstahl, Phys. Rev. Lett. **103**, 082501 (2009).
[24] R. Roth, J. Langhammer, A. Calci, S. Binder, and P. Navratil (2011), 1105.3173.
[25] N. Smirnova, A. D. Maesschalck, A. V. Dyck, and K. Heyde, Phys. Rev. **C69**, 044306 (2004).
[26] R. Bartlett and M. Musiał, Rev. Mod. Phys. **79**, 291 (2007).
[27] O. Jensen, G. Hagen, T. Papenbrock, D. J. Dean, and J. S. Vaagen, Phys. Rev. C **82**, 014310 (2010).

[28] O. Jensen, G. Hagen, M. Hjorth-Jensen, and J. S. Vaagen, Phys. Rev. C **83**, 021305(R) (2011).

[29] S. K. Bogner, T. T. S. Kuo, and A. Schwenk, Phys. Rept. **386**, 1 (2003).

[30] S. K. Bogner, R. J. Furnstahl, S. Ramanan, and A. Schwenk, Nucl. Phys. **A784**, 79 (2007).

[31] D. R. Entem and R. Machleidt, Phys. Rev. C **68**, 041001 (2003).

[32] O. Jensen, G. Hagen, M. Hjorth-Jensen, B. A. Brown, and A. Gade, Phys. Rev. Lett. **107**, 032501 (2011).

[33] V. Somà, T. Duguet, and C. Barbieri (2011), 1109.6230.